Mine Water Environ (2015) 34:320–328
DOI 10.1007/s10230-014-0323-3

TECHNICAL ARTICLE

# Field Research: Measuring Water Pressure Resistance in a Fault-Induced Fracture Zone

De-xian Liang · Zhen-quan Jiang · Yun-zhang Guan

Received: 16 January 2014 / Accepted: 17 December 2014 / Published online: 28 December 2014


**Abstract** Seam floor water-inrush accidents in mine stopes are often associated with fault structures in which water pressure resistance capacities are less than that of the intact seam floor. A new in situ water resistance capacity test was recently developed and used to determine the water resistance properties of a section of a normal fault. The in situ tests defined initial seepage conditions, the state of seepage after flow stabilized, and the measure and calculation of water resistance capability. The test results were used to calculate the unit seepage failure resistance strength, a quantification of the water pressure resistance capacity. It appears that such tests can be used to better evaluate the safety of coal extraction, and whether coal seams under inferred threat from water inrushes can be excavated safely without dewatering or depressurizing the underlying confined aquifers.

**Keywords** In-situ measurement · Water inrush · Permeability

## Introduction

One of the major impacts of groundwater on mining activities is the unpredictable occurrence of water inrush events, in which a significant amount of water suddenly invades an underground mine. Water inrush events occur when the strength of a stratum is not strong enough to resist the water pressure (Zhou and Li 2001). Up to 79.5 % of seam floor water inrush events associated with stope working faces are associated with faults (Bu et al. 2009). These occur when the natural groundwater level is tens or even hundreds of meters higher than the work face, which suggests that the faults are, at least in some circumstances, resisting significant amounts of water pressure (Wu and Fan 2003; Wu and Liu 2003).

The coal seams of the test site lie in the Permo-Carboniferous strata (Fig. 1). The Taiyuan Formation has a thickness of 114–223 m, consisting of argillaceous shale and sandstone. From top to bottom, the coal seams are the 6th coal, 10th bottom coal, 15th upper coal, 16th bottom coal, and 17th coal. The 16th bottom coal and 17th coal seams can be extracted in the entire coalfield, while the others are only distributed in part of it. Except for the lowest two coal seams, which may be hydraulically connected with the underlying 14th limestone and Ordovician limestone, groundwater in the coal seams is generally static, and is relatively easy to dewater or drain. The Shanxi Formation of the Permian system has a thickness of 89 m. It includes two coal seams, the 2nd coal seam and 3rd coal seam. Beneath the Taiyuan Formation is the Benxi Formation, which is 18–86 m thick and consists of limestone, argillaceous shale, and iron ores. The Ordovician limestone, which has an average thickness of 750 m, is a highly permeable confined aquifer. It is a potential threat to mining of the two lower coal seams, which are listed as prospective reserves. So the rock stratum between the 17th coal seam and Ordovician limestone can serve as a geological barrier for preventing Ordovician limestone water from flowing into mines when the 16th bottom coal and 17th coal seams are extracted. But when a fault interrupts this geological barrier, it can act as a water inrush channel. Therefore, the seepage resistance of such a fault is of great importance.

D. Liang (✉) · Z. Jiang
School of Resources and Earth Science, China University of Mining and Technology, Xuzhou 221116, Jiangsu, China
e-mail: tomyleung1986@qq.com

Y. Guan
Yanzhou Coal Mining Co. Ltd, Yankuang Group Co. Ltd, Zoucheng 273500, Shandong, China

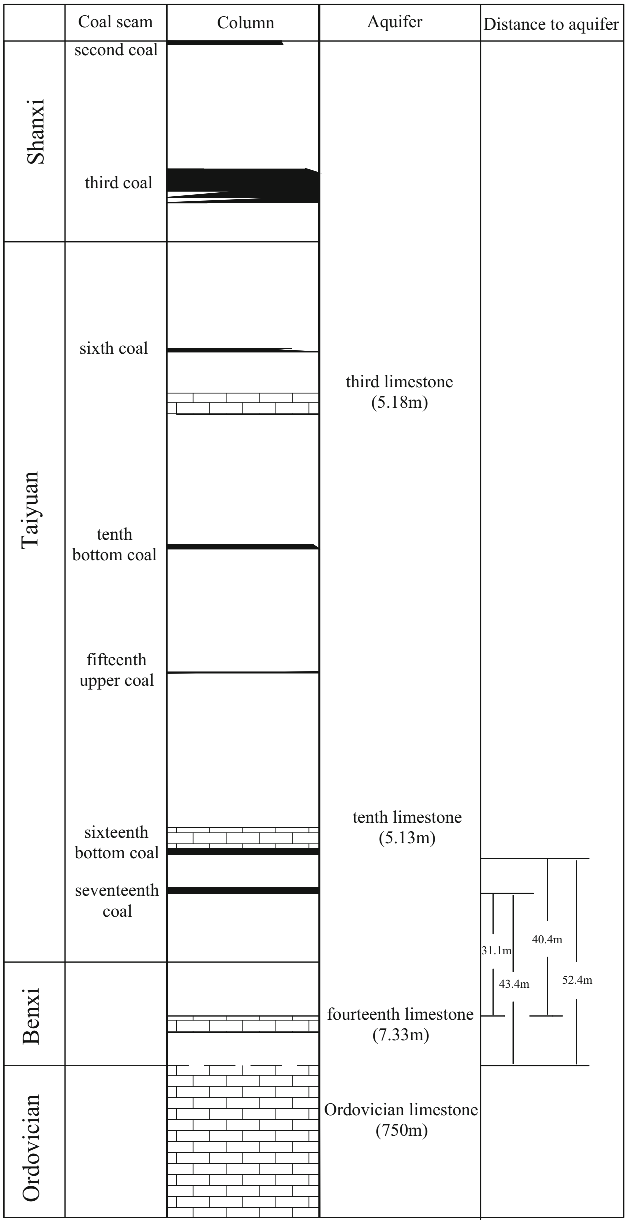


**Fig. 1** The geological column of the Yanzhou coalfield

Because of the great disparity between the natural environment and laboratory conditions, in situ testing of water-pressure resistance is necessary. This paper discusses an in situ test that we developed and tested in a fault fracture zone to establish the fault zone's permeability characteristic parameters and quantify its water-pressure resistance, with the objective of improving mine safety.

## Test Method and Principle

A dual-hole water-pressure method was used to assess resistance (Fig. 2). Two holes, one for injection and another for measurements, were used to measure water pressure and infiltration. The injection hole was drilled in two steps. First, after drilling to the top of the rock stratum to be tested, we attached the casing to the bottom of the hole and used cement grout to seal the gaps between the outer casing wall and the rock. Then, drilling was continued through the test stratum, and a packer was installed at the bottom of the finished hole. The top of the hole was sealed with a flange, where a water supply connector and a water pressure sensor were settled.

The measurement hole was directly drilled through the test stratum and packers were separately installed at the top and bottom of the test stratum. The water pressure sensor of this hole was installed between the two packers and the gap was filled with coarse sand. The top of this hole was also sealed with a flange.

Different injection pressures were used for each 20 min test and the flow rate and water pressure in each hole were continuously recorded. If the seepage pressure changed significantly at one water pressure, the test was stopped at the next higher water pressure. Other key parameters can be calculated or analyzed, including the hydraulic conductivity, water-pressure resistance of the floor stratum, and the effect of water pressure on seepage diversion. Thus, this test allows one to quantitatively evaluate stratum permeability and resistance to seepage failure under natural conditions.

### Initial Seepage Assessment

In order to quantify and evaluate the initial seepage conditions in the test section, we defined the initial seepage point where the water pressure in the test hole and seepage flow obviously changed (Fig. 3). The corresponding water injection pressure for the initial seepage flow is referred to as the initial seepage water pressure ($P_{w0}$). The so-called seepage water pressure is the minimal pressure of the rock formation induced by hydro-fracturing under water pressure and maps to the injection pressure of that test. On the water-pressure process curve, the relevant difference measured at the test hole corresponds to the osmotic resistance to seepage and can serve as the initial water-resistance property of the test section.

### Stable-State Seepage

During the test, we kept increasing the pressure until cracks extension occurred, which was observed as a change in the water pressure. After that, the water pressure in the test hole and seepage flow remains relatively stable (Fig. 3). This level of seepage is defined as the stable seepage and the corresponding maximum stable water pressure is the stable water pressure ($P_s$), with the

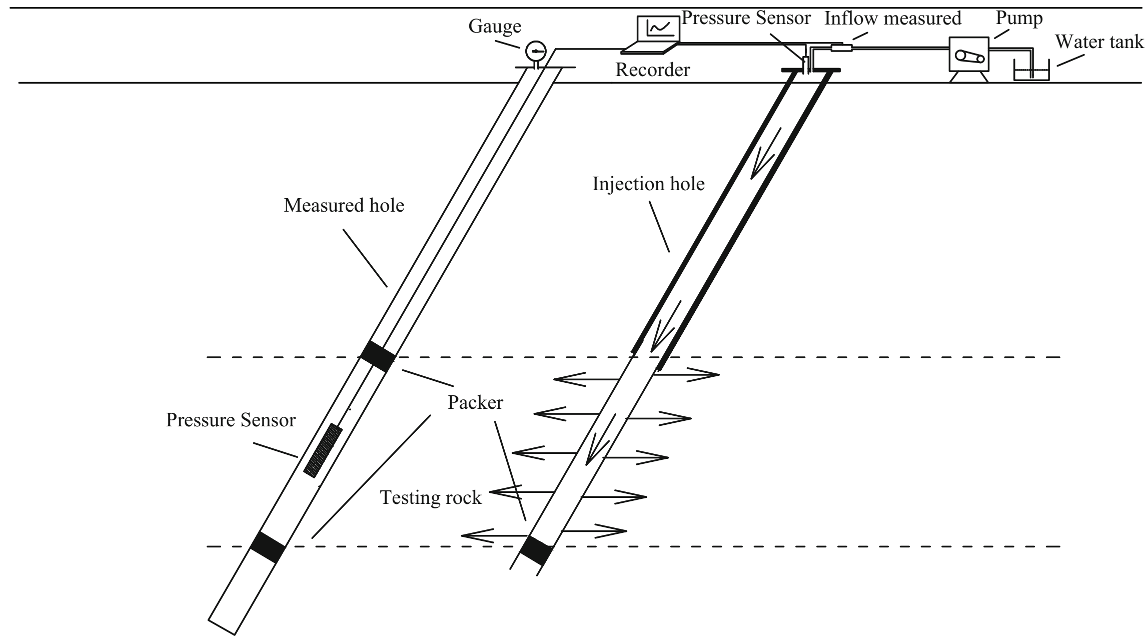


**Fig. 2** Sketch of the water-pressure test device

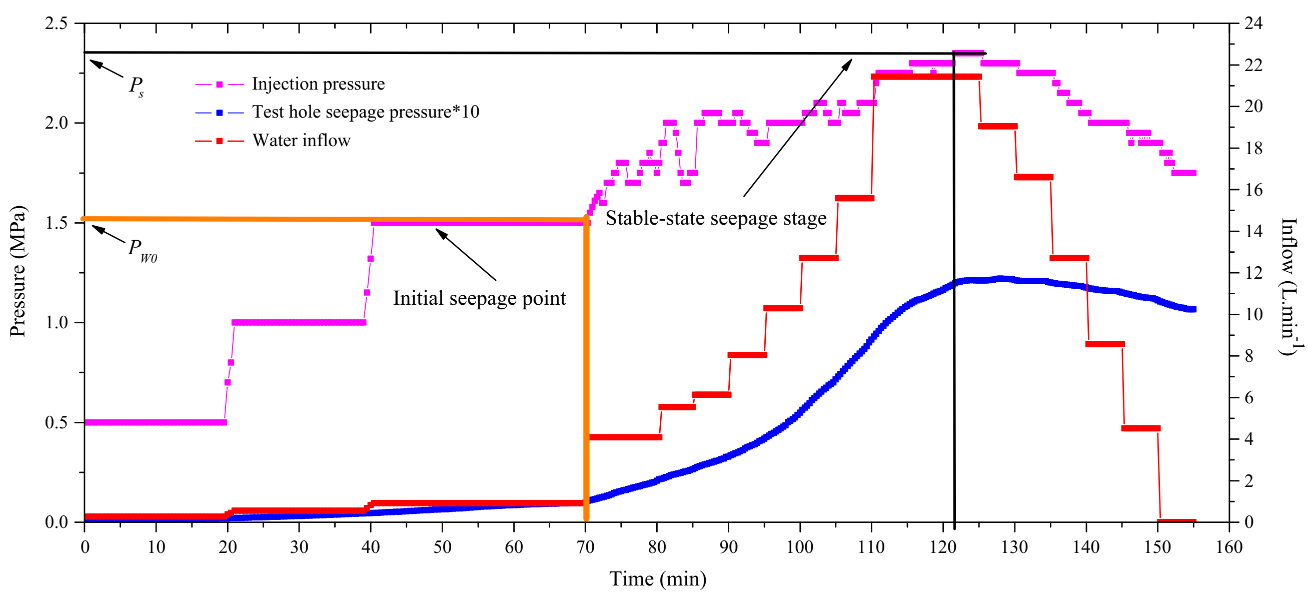


**Fig. 3** Sketch of the initial seepage point and stable-state seepage stage

correlating water pressure of the test hole and seepage flow reflecting the seepage condition of the test section at this water pressure.

## Permeability of the Test Section

The permeability of the test section in a seepage state can be reflected quantifiably, though indirectly, by the permeability coefficient of the seepage process. With the measured water pressure data of the water injection and test hole, one can calculate the hydraulic conductivity of the test hole if it is assumed that the permeability of the test section is isotropic and homogeneity (Fig. 4). However, flow in cracks and faults under high water pressure is turbulent, not laminar, and therefore does not follow Darcy's Law (Jiang et al. 2007, 2010; Miao et al. 2004). When flow and seepage pressure reach a stable state, the flow rate ($Q$) is stabilized. According to the Chezy formula of turbulent flow (Bulut et al. 1996; Guo et al. 2005; Jiang et al. 2007, 2010; Li et al. 2007):

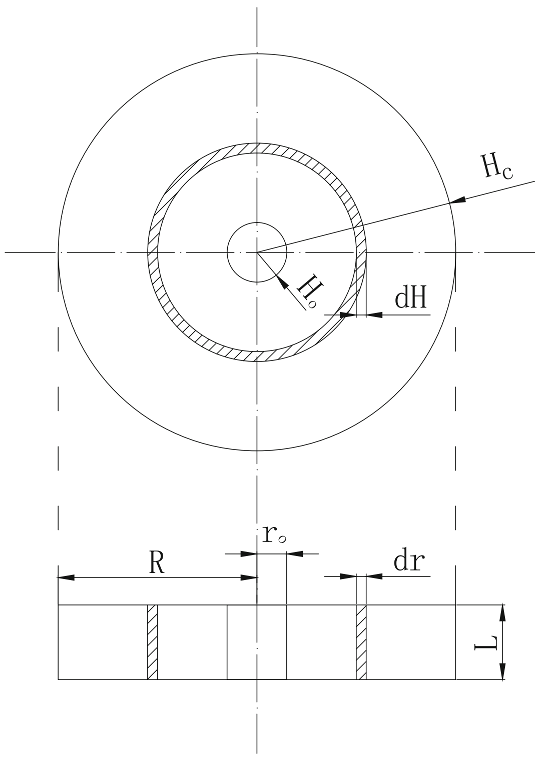


**Fig. 4** The plane of water flow model

$$v = KJ^{1/2} \quad (1)$$

$$Q = 2\pi rKLJ^{1/2} \quad (2)$$

where $v$ is the seepage velocity, m/s; $K$ is the hydraulic conductivity, m/s, $Q$ is the water flow rate, $m^3/s$, $L$ is the length of the test section, m, and $J$ is the hydraulic gradient, which is:

$$J = -\frac{dH}{dr} \quad (3)$$

where $H$ is the water head, m and $r$ is the distance from the water injection point, m.

According to this, water head is:

$$dH = -\left(\frac{Q}{2\pi KL}\right)^2 \frac{dr}{r^2} \quad (4)$$

Formula (4) can be described as:

$$\int_{H_{P_0}}^{H_P} dH = -\int_a^R \left(\frac{Q}{2\pi KL}\right)^2 \frac{dr}{r^2} \quad (5)$$

Thus, hydraulic conductivity can be calculated from the formula:

$$K = \frac{Q}{2\pi L}\left[\frac{R-a}{(H_{p0}-H_p)Ra}\right]^{1/2} \quad (6)$$

where $R$ is the distance between the water pore and test hole, m, $a$ is the test hole radius, m, $H_{P0}$ is the head of water pressure, m, and $H_p$ is the test hole water head, m.

## Water Pressure Resistance of the Test Section

The initial seepage suggests that the flow path for seepage already existed, although there were large differences in seepage strength between the test sections due to the nature of the flow path. Comparing the process curve of initial water pressure and the repeated water pressure tests of each test section, it was found that the initial seepage still required high water pressure. Considering that the cracks for seepage already existed, this continued requirement of high water pressure was attributed to the constraint that deep crustal stress imposes on cracks. This constraint greatly affects the connectivity of the crack passage, dramatically intensifying seepage resistance. This was also reflected by stress–strain and permeability correlation properties measured by a servo-controlled permeability test (Jiang and Ji 2001; Wu and Fan 2003; Wu and Liu 2003). Mining-induced water inrushes through the coal seam floor always happen during the dilation stage when the floor stratum stress is relieved, while the water-pressure test is carried under the original crustal stress. Therefore, the restraint imposed by crustal stress cannot be neglected if the result from an in situ water-pressure test is adopted as an analogy of water pressure resistance.

Quantifying the impact that crustal stress has on underwater seepage has been done theoretically and with relevant field tests (Bai et al. 2009; Haimson 1977; Li et al. 1999, 2002; Yin et al. 2001). Seepage water pressure was measured in repeated water-injection tests to determine how crustal stress and the associated extension cracks constrain hydraulic fracturing. To evaluate seepage failure resistance capacity, we tested the hypothesis that the stratum is the homogeneous isotropic medium and that resistance of the extension cracks can provide the quantitative basis of seepage resistance intensity of the stratum. Once the rock surrounding a borehole is broken, as long as enough water is injected, cracks will extend in the direction of least resistance. The mechanics model of crack surface extension is shown in Fig. 5; cracks extend only if the water pressure is equal or exceeds the sum of the minimum principal stress and the seepage failure extending resistance. So,

$$P_s = P_f + \sigma_0 \quad (7)$$

$$\sigma_0 = \lambda\sigma_z = \lambda\gamma \mathrm{H} \quad (8)$$

$$\lambda = \frac{v}{1-v} \quad (9)$$

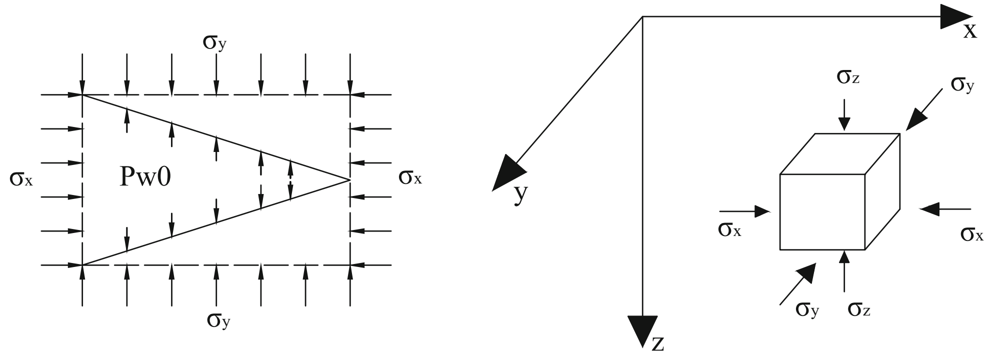


**Fig. 5** Mechanical model of crack surface extension

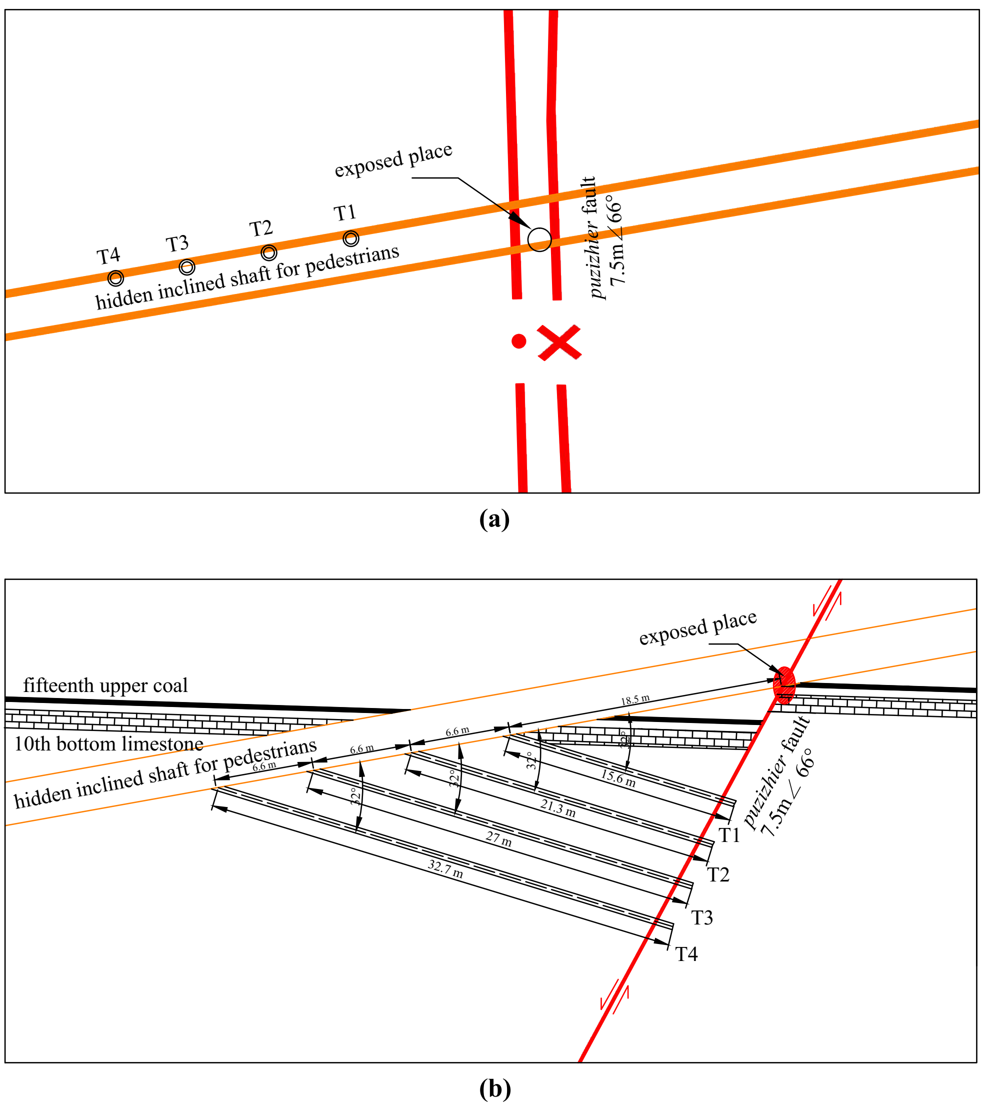


**Fig. 6** Test holes layout diagram. **a** Plane, **b** Profile

where $P_f$ is the seepage failure extending resistance, Kpa, $P_s$ is the stable water pressure in the water-injection test, Kpa, $\sigma_0$ is the constraint of crustal stress (the minimum principal stress), Kpa, $\lambda$ is the lateral pressure coefficient, $\sigma_z$ is gravity stress, Kpa, $\gamma$ is the average specific weight of the overlying rock, KN/m$^3$, $H$ is the thickness of the overlying rock, m, and $\nu$ is the Poisson ratio.

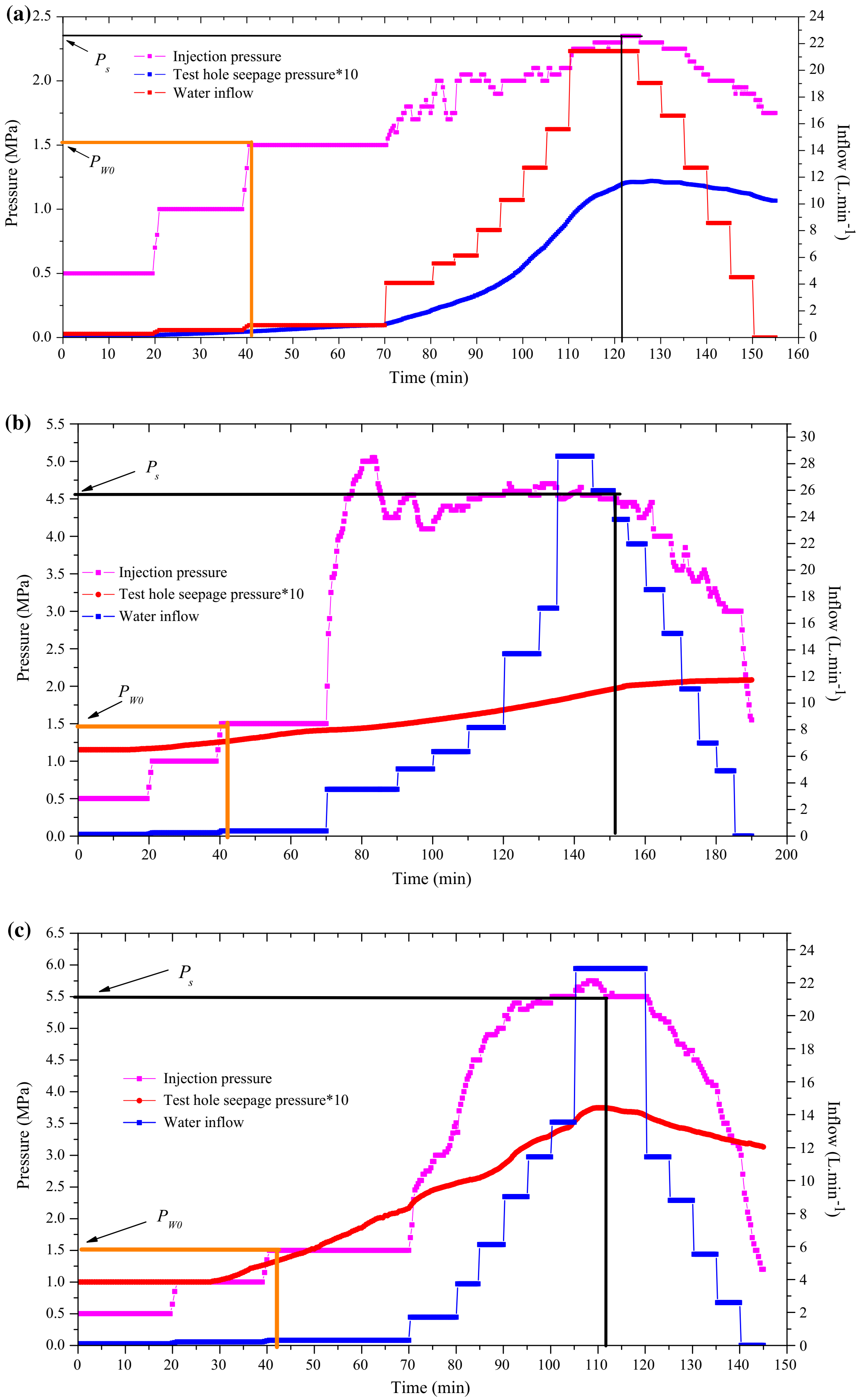


**Fig. 7** Curve of the water-pressure process. **a** First section, **b** second section, **c** third section

Thus, the intensity, $P_0$, of the unit stratum seepage failure extending resistance can be defined as a stratum's water-pressure per average meter of thickness, while the intensity of the water-pressure resistance of the extension cracks is numerically equal to the seepage water pressure in repeated water-pressure tests with the constraint impact of crustal stress deducted. The formula for calculating the water-pressure resistance intensity can be described as:

$$P_0 = \frac{P_f}{L} = \frac{P_s - \sigma_0}{L} \quad (10)$$

where $P_0$ is the water-pressure resistance intensity, Kpa/m. It is theoretically appropriate to use this method since the test conditions and the result of the water-pressure test are similar to hydro-fracturing crustal stress tests. Despite potential errors from various technical and human factors, it appears that our measured results can reflect the actual seepage failure resistance characteristics of the rock well.

## Engineering

### Engineering Layout

Field measurements were carried out in a section of a hidden inclined shaft for pedestrians (a kind of inclined channel) where a fault was exposed, to test the seepage resistance of the mine's *puzizhier* fault (Fig. 6). A *puzizhier* fault is a normal fault with about a 7.5 m fall, with a 66° dip angle of the fault surface, and a 0.7 m wide crushed zone. The inclined shaft is in the fault-induced fracture zone and about 25 m from the 10th bottom limestone (Carboniferous) aquifer. According to the drilling methods described earlier, four holes (Z1, Z2, Z3, and Z4) were drilled through the fault crushed zone. The angle between the holes and the inclined shaft was 32° and the fault-crushed zone was divided into three sections by these four holes. In order to decrease the impact of the water pressure test on the 10th bottom limestone aquifer, each test hole crossing the fault-induced fracture zone was kept a certain distance from it. The four holes served as injection holes and measurement holes alternately. Thus, Z1 was used for injection and Z2 for measurements hole the test of the first section, Z2 was the injection hole and Z3 was a measurement hole during the second section's test, and Z3 was an injection hole and Z4 was a measurement hole during the third section's test. These four test holes were subsequently used to monitor water pressure disturbance in the fault after the test, with each test hole a certain distance from the fault-exposed section during shaft development.

### Analysis of Initial Seepage Condition

The initial seepage water pressure of the three test sections, as well as the relevant parameters of the seepage condition was defined using the measured data (Fig. 7; Table 1). Although there was initially no flow in the *puzizhier* fault, the seepage resistance was relatively weak. The initial seepage water pressure was about 1.5 Mpa and its pressure gradient was around 0.4 Mpa/m. Although the seepage water pressure of the fault fracture is quite low, it still had a high seepage pressure difference (almost 1.5 Mpa). This indicates that tiny seepage channels can cause high water resistance.

### Analysis of Stable-State Seepage Conditions

The stable-state seepage parameters of the three test sections of the *puzizhier* fault can be obtained from the measured data (Fig. 7; Table 2). Stable-state seepage does not mean structural destruction has taken place in the stratum but continual seepage does indicate partial crushing. The measured results show that the *puzizhier* fault does not initially have seepage and that the initial seepage water

**Table 1** Measured water pressure of initial seepage, Mpa

| Test section | Initial seepage water pressure ($P_{w0}$) | Test hole water pressure | Seepage pressure difference | Water pressure gradient, Mpa/m |
|---|---|---|---|---|
| First section | 1.52 | 0.03 | 1.49 | 0.42 |
| Second section | 1.45 | 0.12 | 1.33 | 0.38 |
| Third section | 1.5 | 0.13 | 1.37 | 0.40 |

Distance between water injection hole and test hole is 3.5 m

**Table 2** Measured water pressure of stable-state seepage, Mpa

| Test section | Stable water pressure ($P_s$) | Test hole water pressure | Seepage pressure difference | Water pressure gradient, Mpa/m |
|---|---|---|---|---|
| First section | 2.3 | 0.12 | 2.18 | 0.62 |
| Second section | 4.6 | 0.21 | 4.39 | 1.25 |
| Third section | 5.75 | 0.34 | 5.41 | 1.55 |

Distance between water injection hole and test hole is 3.5 m

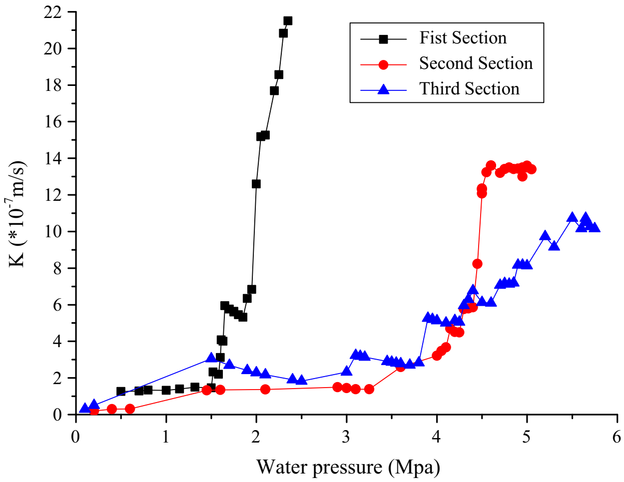


**Fig. 8** Permeability changes for the three sections

pressure of these three test sections is similar, about 1.45–1.52 Mpa. However, compared with the water pressure for stable-state seepage formation, the water pressure resistance of the first section is comparatively low (2.3 Mpa), far below (4.6 and 5.75 Mpa, respectively) that of the last two sections. This difference is attributed to the first section being located in the shallow part (vertical depth less than 10 m) of the inclined pedestrian shaft. Tunneling disturbed the first test section and reduced water resistance intensity, although no active seepage was caused.

### Permeability Changes

Hydraulic conductivity was calculated according to Eq. 6. Figure 8 shows that the calculated hydraulic conductivities of the three sections range from $1.26 \times 10^{-7}$ to $21.5 \times 10^{-7}$ m/s, $0.21 \times 10^{-7}$ to $13.6 \times 10^{-7}$ m/s, $0.32 \times 10^{-7}$ to $10.3 \times 10^{-7}$ m/s, respectively. The conductivity of the three sections changed similarly. Initially, while the water injection pressure was relatively low, hydraulic conductivity was not significantly affected by increases in water pressure. Then, as water pressure was increased, the first increase in hydraulic conductivity occurred when a water pressure that could force crack extensions was reached. Finally, seepage arrived at a stable-state as water pressure was further increased; the hydraulic conductivity sharply increased as cracks extended further.

### Water Pressure Resistance Intensity Calculation

The test section is located at a depth of 460 m with a length of 3.5 m. According to Eqs. 7–10, the overlying strata gravity stress is 10 Mpa, with 4.2 Mpa of the crustal constraint impact stress (lateral pressure coefficient, $\lambda$, of the structural disturbance area is 0.42, converted by Poisson's ratio, $v$, to between 0.28 and 0.3). The stable water pressure was 4.6 Mpa, which was calculated from the third repeated water-pressure measurement. Thus, the corresponding water pressure resistance intensity is 0.11 MPa/m. The calculation process is shown:

$$\lambda = \frac{v}{1 - v} = \frac{0.296}{1 - 0.296} \approx 0.42$$

$$\sigma_0 = \lambda \gamma H = 0.42 \times 21.7\,\mathrm{KN/m^3} \times 460\,\mathrm{m} \approx 4200\,\mathrm{Kpa} = 4.2\,\mathrm{Mpa}$$

$$P_0 = \frac{P_s - \sigma_0}{R} = \frac{4.6\,\mathrm{Mpa} - 4.2\,\mathrm{Mpa}}{3.5\,\mathrm{m}} \approx 0.11\,\mathrm{Mpa/m}.$$

## Conclusions

The water pressure resistance capability of a fault can be quantitatively evaluated by an in situ water-pressure test. Initially, hydraulic conductivity weakly correlates with increased water pressure because the water injection pressure is far from that required to extend cracks. Hydraulic conductivity increases sharply until the water pressure is sufficient to do this. Mining induced water inrushes from the coal seam floor always happen at the dilation stage. Therefore, the restraint imposed by crustal stress must be subtracted from the water injection pressure if the measured result from an in situ water-pressure test is adopted as the analogous evaluation of water pressure resistance. For the test case, near the test site, where coal seams and confined aquifers were connected by the *puzizhier* fault, the water pressure per average meter of thickness must be kept below the water-pressure resistance, 0.11 Mpa/m, to keep the coal mine safe. Utilization of this test could allow coal seams under inferred threat from such water inrushes to be excavated safely without dewatering or depressurizing the underlying confined aquifers.

**Acknowledgments** The authors thank the State Basic Research and Development Program of China (No. 2013CB036003) for funding this study. Special thanks to Huang Zhen and our partners who collected data in the field test.

## References

Bai HB, Mao XB, WU Yu, Chen ZQ (2009) Research on water-reserved mining with high water pressure under large-scale thrust-fault in Ordovician karsts. Chin J Rock Mech Eng 28(2):246–252

Bu WK, Mao XB (2009) Research on effect of fault dip on fault activation and water inrush of coal floor. Chin J Rock Mech Eng 28(2):386–394 [in Chinese, abstract in English]

Bulut F, Boynukalm S, Tarhan F, Dilek R (1996) A new approach to the evaluation of water-pressure test results obtained in bedrock by the US Bureau of reclamation method. Eng Geol 44(1):235–243

Guo QL, Wang HZ, Zhang ZG (2005) Study of permeability character under high water pressure in the surrounding rock of the air-cushion surge tank in the *Xiaotiandu* hydropower station. J Hydroelectr Eng 24(1):102–106

Haimson BC (1977) Crustal stress in the continental United States as derived from hydrofracturing tests. Geophys Monogr Ser 20:576–592

Jiang ZQ, Ji LJ (2001) The laboratory study on behavior of permeability of rock along the complete stress-strain path. Chin J Geotech Eng 23(2):153–156

Jiang ZM, FU S, LI SG, Hu DK, Feng SR (2007) High pressure permeability test on hydraulic tunnel with steep obliquity faults under high pressure. Chin J Rock Mech Eng 26(11):2318–2323

Jiang ZM, Feng SR, Fu S, Chen SH (2010) Test study of osmotic behavior of fractured rock mass of water tunnel under high water pressure. Rock Soil Mech 03:673–676

Li JX, Li DP, Zhang WQ, Liu WT (1999) The relations of initial geo-stress and water irruption of seam floor [J]. Chin J Rock Mech Eng 18(4):419–423

Li XZ, Luo GY, Chen ZS (2002) The mechanism of deformation and water conduction of fault due to excavation in water inrush in underground engineering. Chin Geotech Eng 24(6):695–700

Li P, Lu WX, Long YQ, Yang ZP (2007) Seepage analysis in a fractured rock mass: the upper reservoir of the *Pushihe* pumped-storage power station in China. Eng Geol 97(1):53–62

Miao XX, Liu WQ, Chen ZQ (2004) Dynamics of systems of seepage flow in surrounding rock affected by mining. Science Press, Beijing

Wu JW, Fan C (2003) Study on in situ measurement of water-resisting ability of coal seam floor rock mass. Chin Geotech Eng 25(1):67–70 [in Chinese, abstract in English]

Wu JW, Liu XH (2003) In-situ measurement study and evaluation on water-resisting ability of rock mass in fault zone. Rock Soil Mech 24(10):447–450 [in Chinese, abstract in English]

Yin JM, Chen LW, Zhong ZW, Feng J, Guo L (2001) Measurement and interpretation on in situ stresses with hydro-fracturing in a highway tunnel site. Chin J Rock Mech Eng 20(1):1827–1830

Zhou WF, Li GY (2001) Geological barrier-a natural rock stratum for preventing confined karst water from flowing into mines in North China. Environ Geol 40:1003–1009